IEEE Access
Multidisciplinary | Rapid Review | Open Access Journal

Received November 13, 2018, accepted December 5, 2018, date of publication December 14, 2018,
date of current version January 7, 2019.

Digital Object Identifier 10.1109/ACCESS.2018.2886823

KSVD-Based Multiple Description Image Coding

GUINA SUN, LILI MENG, LI LIU, YANYAN TAN, JIA ZHANG, AND HUAXIANG ZHANG
School of Information Science and Engineering, Shandong Normal University, Jinan 250014, China
Institute of Data Science and Technology, Shandong Normal University, Jinan 250014, China

Corresponding author: Lili Meng (mengll_83@hotmail.com)

This work was supported in part by the National Natural Science Foundation of China under Grant 61572298, Grant 61601269, Grant 61602285, Grant 61601268, and Grant 61702310 and in part by the Natural Science Foundation of Shandong China under Grant ZR2016FB12.

ABSTRACT In this paper, we present a new multiple description coding scheme, which is based on a sparse dictionary training method called K singular value decomposition (KSVD). In the proposed scheme, each description encodes one source subset with a small quantization stepsize, and other subsets are predictively coded with a large quantization stepsize. The source processed by the KSVD becomes sparse, which can improve the coding efficiency. The proposed scheme is then applied to lapped transform-based multiple description image coding. Finally, image coding results show that the proposed scheme achieves a better performance than the current state-of-the-art multiple description coding methods.

INDEX TERMS K singular value decomposition (KSVD), multiple description coding, sparse representation.

I. INTRODUCTION

With the development of communication technology, the transmission of information on the network is more and more frequent. But the internet and wireless communication networks are unreliable, which can result in bit error, packet loss, or delay. To solve these issues, multiple description coding (MDC) [1] emerges and gradually becomes a mainstream technology applied in harsh channel conditions. It partitions the source into multiple bit streams and transmits them through different channels respectively, which can reduce the probability of all data being lost at the same time. These bit streams are called description and they are equally important. When one description is received, the image can be restored roughly. And if more descriptions can be received, the recovered image quality is better.

The multi-description idea was proposed by Bell Labs in the 1970s [2]. The first MDC method is putted forward by Vaishampayan, called multiple description scalar quantization (MDSQ) [3], which generates two sub-streams by producing two indices for each quantization level. It is a multiple description design focusing on scalar quantization system.

In [4] and [5], some extension methods of MDSQ for more than two channels are proposed, which employ a combinatorial optimization approach to divide the multiple description system into multiple stages. In [6] and [7], a lattice vector quantization-based MDC (MDLVQ) method is presented, which generates M descriptions by using M-fraction lattice to regularly divide the fine lattice. But all of them will lead to complex index allocation problems as M increases.

In [8], a design of MDC scheme based on wavelet transform considering the use of pairwise correlating transform (PCT) is proposed. It divides the coefficients of discrete cosine transform (DCT) transform into two groups and introduces correlation through a linear transformation. When one is lost, it can be estimated from another received by the correlation between two groups. And many related improvements for MDC based on wavelet transform are developed [9]–[11]. In [12], a new technique that produces multiple description by quincunx spatial multiplexing is studied. It employs a multiphase downsampling for input image and uses a local random binary convolution kernel to replace the traditional low-pass filter.

In [13], it presents a novel multiple description lapped transform with prediction compensation (MDLTPC) for two-description, which encodes one subset as the base layer and encodes the prediction residual of other subset as the enhancement layer in same description. In [14], a M-channel MDC scheme using two-rate predictive coding and staggered quantization (TRPCSQ) is proposed, where the prediction residuals are encoded by $M-1$ lower-rate uniform quantizers in different descriptions. In [15], an extension method three-layer MDC (TLMDC) is developed to refine the low-rate-coded subsets. If receiving more than two low-rate

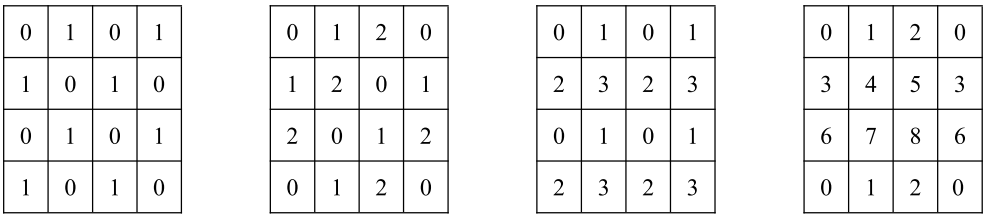

FIGURE 1. Block subset definitions in MD image coding. (a) M = 2; (b) M = 3; (c) M = 4; (d) M = 9.

reconstructions of a subset, it uses their average as the final reconstruction.

Recently, two more effective MDC methods with randomly offset quantizers (MDROQ) and uniformly offset quantizers (MDUOQ) are proposed [16] by generalizing the random and uniform quantization theory [17]. The MDROQ method has random offsets due to predictive coding, which refines the optimal reconstruction of intersection of all received quantization bins as the final reconstruction. The MDUOQ method has near-uniform offsets among different low-rate quantizers because the unequal deadzones are used in different quantizers.

Since the image is complex two-dimensional signal, a single orthogonal transformation base does not fully reflect the geometric characteristics of the image. In the previous methods, they usually adopt DCT orthogonal transform that lost some details of the image. Later, some works on the image transformation methods are studied [18], [19]. Reference [20] obtains ultra-fine description granularity by locally adaptive sparse representation of video signals. In this paper, we focus on sparse representation of image and present the KSVD-based MD image coding scheme, which adopt the redundant dictionary trained by KSVD to replace the orthogonal base dictionary obtained by DCT.

The rest of paper is structured as follows. In Section II, some related works are introduced. In Section III, the system model is described, and a new transformation is formulated. Simultaneously, the advantages of the proposed scheme are analyzed. Next, in Section IV, simulations are performed to verify the effectiveness of proposed schemes. Finally, Section V concludes the whole paper.

II. RELATED WORKS

A. MDROQ AND MDUOQ METHODS

In [16], two MDC methods are proposed, based on prediction-induced randomly offset quantizers and unequal-deadzone-induced near-uniformly offset quantizers, respectively. They introduce deadzone quantizer based on the TRPCSQ method, which have better rate-distortion (R-D) performance than just using uniform quantizer. In both methods, they partition the input image into M subsets using some two-dimensional patterns as show in Fig. 1 to derive M descriptions.

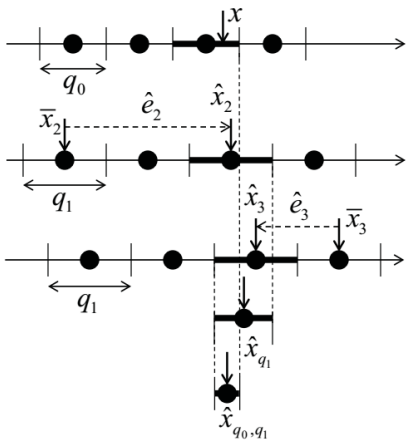

FIGURE 2. A three-description coding example of joint de-quantization from prediction-induced random quantizers.

Each description is generated by employing a uniform or deadzone scalar quantizer to encode M subsets. First, it uses the time-domain lapped transform (TDLT) [21], [22] to improve the coding efficiency. It adds a pre-filter before the block transform and a post-filter after the inverse transform.

Then, for the i-th description, the i-th subsets is encoded with a small quantization stepsize q_0, and other subsets are predicted in turn based on the block transform coefficients of previously encoded subsets. After that, it calculates the prediction residuals and encodes them with a quantization stepsize q_1, where $q_1 > q_0$. The prediction and the calculation of the prediction residuals are obtained by using the DCT-domain Wiener filter [23], [24].

At last, at the decoder, each sample is reconstructed jointly from all received descriptions, based on the intersection of all received quantization bins. The reconstruction of sample x in the i-th description is:

$$\hat{x}_i = \bar{x}_i + \hat{e}_i. \tag{1}$$

$\bar{x}_i$ is the prediction of x in the i-th description, $\hat{e}_i$ is the reconstruction value of the corresponding prediction residual e_i.

The MDROQ method is based on prediction-induced randomly offset quantizers. Fig.2 shows a reconstructed three-description example. Where x is original sample in

description 0. It can be seen that the quantization bins that x belongs to in different descriptions are randomly offset because the random predicting $\bar{x}_i$. According to all received descriptions, it refines the optimal point of the intersection of quantization bins as the reconstructed sample, e.i. $\hat{x}_{q_0,q_1}$.

The MDUOQ method is based on unequal-deadzone-induced near-uniformly offset quantizers. It uses quantizers of unequal deadzone sizes to derive the initial uniformly offset quantizers. Fig.3 lists a example of uniformly offset quantizers with unequal deadzone for $M = 3$. Where (a) and (b) are the original quantizers with unequal-deadzone-induced uniform offsets. Through the quantized prediction, quantizer (c) is obtained by shifting to $3q_1$ from quantizer (a) and quantizer (d) is obtained by shifting to $-2q_1$ from quantizer (b).

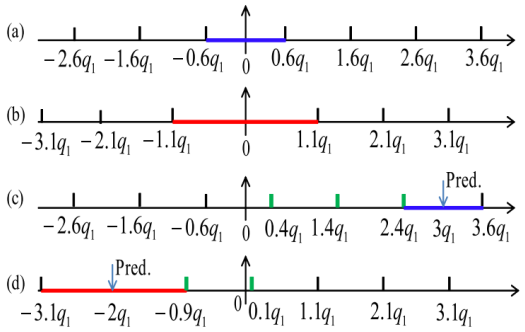

FIGURE 3. Examples of uniformly offset quantizers with unequal deadzone and $\delta = 0.6$ and $M = 3$.

B. KSVD ALGORITHM

Elad proposed the KSVD algorithm in 2006 [25], which generalizes the K-means clustering process. It trains an overcomplete dictionary by alternately performing between sparse coding and updating the dictionary atoms to better represent data. The dictionary trained by the KSVD performs well for both synthetic and real images in applications.

When giving a training set $Y = \{y_i \in R^m\}_{i=1}^N$, it can find the optimal dictionary D with K atoms to sparsely represent Y by solving the following optimization problem:

$$\min_{D,X}\{\|Y - DX\|_F^2\} \quad subject\ to \quad \forall i, \|x_i\|_0 \le T_0. \tag{2}$$

where $D \in R^{m\times K}(K \gg m)$, $X \in R^{K\times N}$ is the sparse code of Y, and T_0 is a threshold of the sparsity of X. This algorithm is as follows:

Firstly, setting the initial dictionary matrix $D_0 \in R^{m\times K}$ with l^2 normalized columns.

Then, repeating the following two stages until convergence:

- *Sparse coding stage:* it computes the corresponding representation vectors x_i of each example y_i using any pursuit algorithm, just like Matching Pursuit (MP) [26] or Orthogonal Matching Pursuit (OMP) [27], [28]. Kaur and Budhiraja [29] demonstrates OMP has faster recovery for images compared with the least squares method, and the OMP is easily implemented and is faster. Thus, we choose OMP algorithm in this paper. The best sparse code X can be got by:

$$X = \arg\min_{x_i} \|y_i - Dx_i\|_F^2 \quad subject\ to \quad \forall i, \|x_i\|_0 \le T_0. \tag{3}$$

- *Dictionary updating stage:* it only updates one column of D at a time via solving a small singular value decomposition (SVD) problem:

$$E_k = Y - \sum_{j\neq k} d_j x_T^j. \tag{4}$$

$$E_k^R = U\triangle V^T. \tag{5}$$

where E_k is the overall representation error matrix, E_k^R is restricted matrix of E_k and x_T^j is the j-th row of X (this is the coefficients corresponding to the j-th column of D). The first column of U as the updated column of D, and the first column of V multiplied by $\triangle(1, 1)$ updates the corresponding coefficient vector.

III. THE PROPOSED SCHEMES

In this section, we mainly describe the KSVD-based MD image coding for $M = 2, 3, 4$ *and* 9. Firstly, the proposed block transform based on KSVD algorithm is presented. Then, the MDC system with the KSVD transform is described detailed. Finally, theoretical analysis is given.

A. KSVD-BASED TRANSFORM

Comparing with DCT, the KSVD-based transform can achieve the sparse representation for the source, and reduce the bit rates at the same source quality.

The [25] gives the training redundant dictionary method based on singular value decomposition. The transform coefficients obtained using the constructed dictionary as the transform base are sparse. Therefore, in this paper, we use the sparse transformation based on KSVD rather than DCT for the block transform. The KSVD-based sparse transformation is shown in Fig. 4. We first run the KSVD algorithm to derive the redundant dictionary, and then the image blocks are sparsely transformed to get the sparse transform coefficients.

1) Training sample set: it is a set of N examples of block patches of size 4×4 pixels, where $N = 40000$, the block patches can also be 8×8, 16×16, or 32×32. This is selected randomly from given training images.
2) Test sample set: it is a set of block patches with the same size of the training sample. It is non-overlapping sampled from the test image.
3) KSVD training: we apply the KSVD algorithm to train a redundant dictionary D of size $m \times K$, where m is the dimension of example, $m = 16$ and $K = 64$ in this paper.
4) Sparse transform: the forward transform expression is follow:

$$X = D^{-1}B. \tag{6}$$

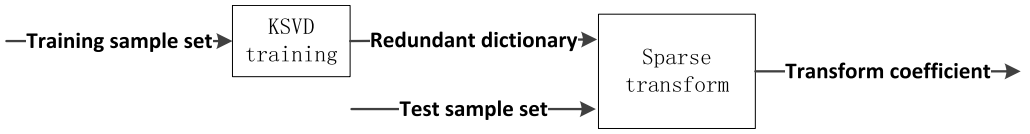

FIGURE 4. The process of KSVD-based transform.

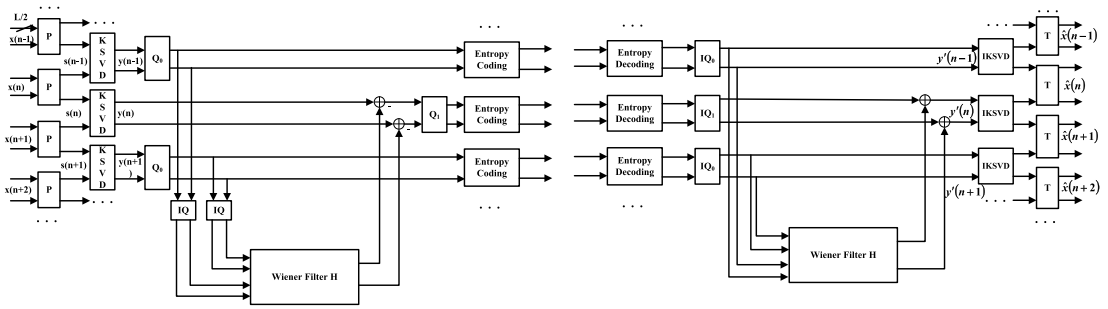

FIGURE 5. Encoder and decoder of KSVD-based MDROQ with $M = 2$.

where B represents the test sample set, and X is the transform coefficient matrix.

The corresponding inverse transformation is:

$$B = DX. \tag{7}$$

B. SYSTEM DESCRIPTION OF KSVD-BASED MDROQ

The system diagram of KSVD-based MDROQ for encoder and decoder of one description with $M = 2$ is shown in Fig.5. Where the block size is $L = 8$ and each line represents half block, i.e., $L/2$ samples. P is a prefilter at the encoder and T is a postfilter at the decoder, which both are used at the boundary of two blocks. Where P and T have the following structures in order to derive a near optimal linear phase overlap transformation:

$$P = Wdiag\{I, V\}W. \tag{8}$$

$$T = P^{-1} = Wdiag\{I, V^{-1}\}W. \tag{9}$$

$$W = \frac{1}{\sqrt{2}}\begin{bmatrix} I & J \\ J & -I \end{bmatrix}. \tag{10}$$

I is an $L/2 \times L/2$ identity matrix, V is an $L/2 \times L/2$ invertible matrix, and J is an $L/2 \times L/2$ counter-identity matrix.

For the MD image coding, to generate M descriptions, we first partition the input image into M subsets. At the encoder, each subset is filtered through P and KSVD-based transformed. The KSVD-based transform make the transform coefficients be sparse. Where $y(i)$ is the corresponding transform coefficients of the i-th subset. Take 2-description as an example, the two subsets $[S_0, S_1]$ can be got by the Fig. 1(a). In description 0, $y(0)$ is encoded with small quantization stepsize q_0 directly; $y(1)$ is predicted from the reconstructed $y(0)$ in all directions and the prediction residuals of $y(1)$ are encoded with a large quantization stepsize q_1. In description 1, $y(1)$ is encoded with small quantization stepsize q_0 directly; $y(0)$ is predicted from the reconstructed $y(1)$ in all directions and the prediction residuals of $y(0)$ are encoded with a large quantization stepsize q_1.

At the decoder, the received descriptions sequential apply entropy decoding and the inverse quantization (IQ). If description 0 is received, the value of IQ of the subset S_0 directly executes the inverse KSVD (IKSVD) transform and postfilter (T) to finish the reconstruction. The value of IQ of S_1 is first adds the value predicted from the reconstructed S_0 and then executes the IKSVD and T. We can reconstruct a rough but acceptable image information. Thus, if more descriptions are received, the quality of restored image will be higher.

The process of encoder and decoder of three-description is shown in Fig.6. It's clearly seen that the prediction sequence of one description obtained for 3-description. In description 0, S_0 subset is encoded directly; S_1 subset is predicted from the reconstructed S_0 subset; S_2 subset is predicted from the reconstructed S_0 subset and S_1 subset.

C. SYSTEM DESCRIPTION OF KSVD-BASED MDUOQ

The framework of KSVD-based MDUOQ for $M = 2$ is similar to Fig.5, in addition to using low-rate quantizers with different deadzones to quantize the prediction.

At the encoder, we employ the KSVD-based transform to obtain the sparse transform coefficients after the prefilter P. Then, the i-th subset is encoded with a quantization stepsize q_0 in the i-th description. Moreover, other subset $j \neq i$ is predicted sequentially and the prediction is quantized with a uniform quantization stepsize q_1. At last, the prediction residual is encoded with a deadzone size of $2(\delta + \frac{l}{M-1})q_1$. Where $2\delta q_1$ is the smallest dedzone size, $l = mod(j - i - 1, M)$.

At the decoder, if the i-th description is received, entropy decoding and the inverse quantization (IQ) are executed first.

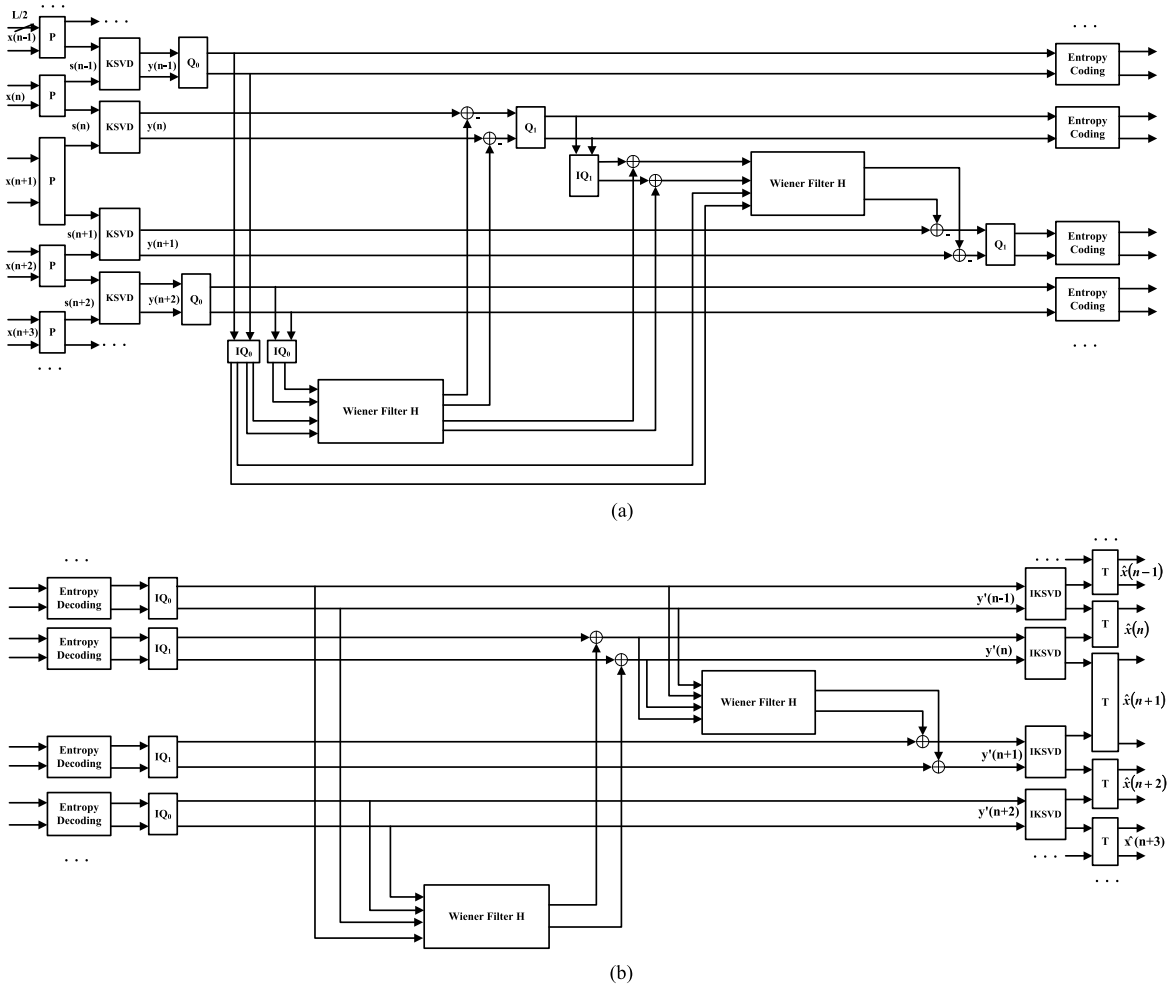

FIGURE 6. Encoder and decoder of KSVD-based MDROQ with $M = 3$. (a) Encoder of one description; (b) Decoder of one description.

Then, the prediction and the prediction residual of subset $j \neq i$ are reconstructed by a uniform quantizer and a deadzone quantizer, respectively. At last, the inverse KSVD (IKSVD) transform and postfilter (T) are used to obtain the reconstruction.

D. THEORETICAL ANALYSIS AND EXPECTED DISTORTION EXPRESSION

In the proposed scheme, the compression of the image is achieved through sparse transformation. Therefore, the sparse transform base has become the key to determine the image compression ratio and image reconstruction accuracy. As the sparsity increases, the complexity of decoding will decrease and the reconstruction of the image will be improved [30]. In this paper, we choose the KSVD-based transform to make the sparse transform coefficients have higher sparsity.

According to the random quantization theory, the closed-form expression of the expected distortion for the proposed MDC scheme is written as:

$$D_E = \sum_{k=0}^{M} p_k e_k. \tag{11}$$

$$p_k = \binom{M}{k} p^{M-k}(1-p)^k. \tag{12}$$

$$e_k = \frac{1}{M}(k e_{0,k} + (M-k)e_{1,k}). \tag{13}$$

where p_k is the probability of received k descriptions, e_k is the corresponding mean squared error (MSE), $e_{0,k}$ is the MSE of subsets with one high-rate and $k-1$ low-rate codings, and $e_{1,k}$ is the MSE of subsets with k low-rate codings.

IV. EXPERIMENTAL RESULTS

We choose six 512×512 standard test images with various characteristics, which are lena, boat, baboon, couple, peppers and goldhill, respectively. They obtain the corresponding sparse transform coefficients through the KSVD-based transform. We adjust the q_0 and q_1 to maintain the same total rate (R) in the simulation experiment and the PSNR value is usually used to measure the quality of recovered image. The larger the value of PSNR, the less distortion the image has.

For the two-description image coding, we compare the performance of KSVD-based MDROQ method with MDROQ [16] and MDLTPC [13]. The results are showed

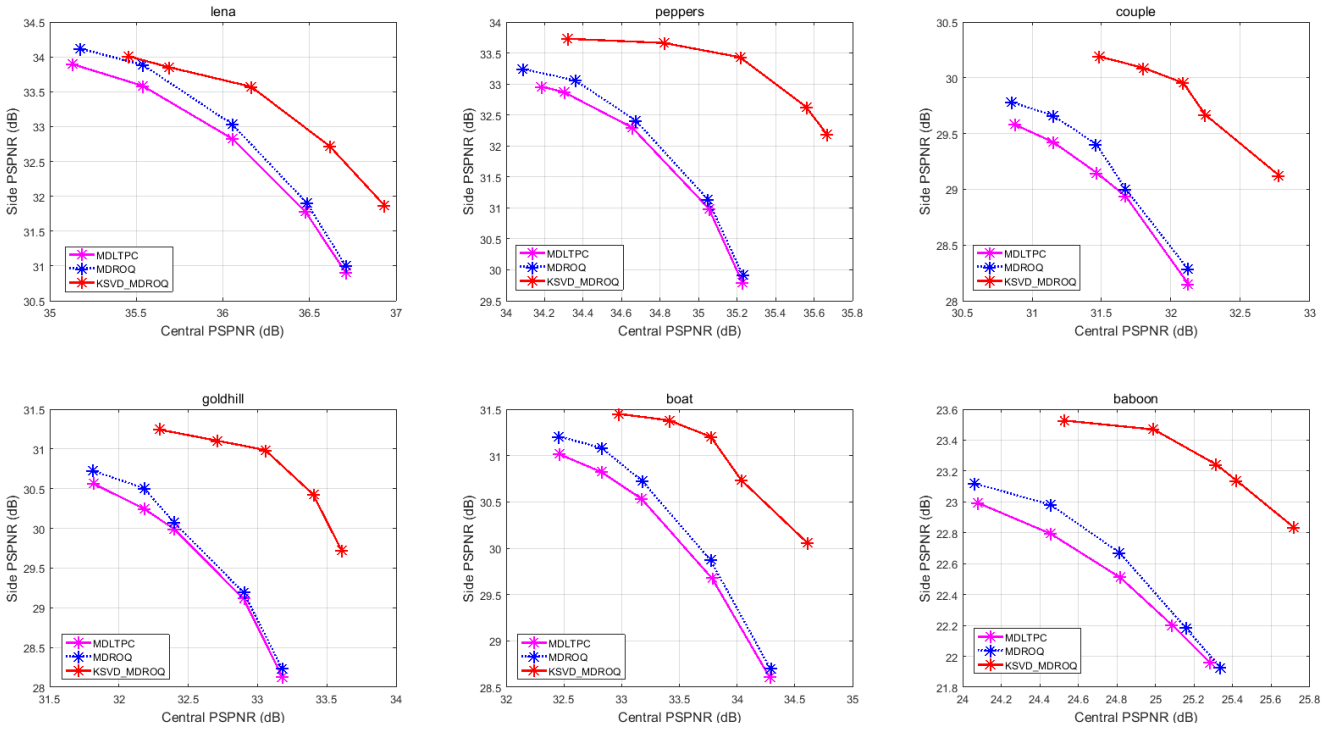

FIGURE 7. The side PSNR and central PSNR of KSVD-based MDROQ, MDROQ and MDLTPC for $R = 0.5$ *bpp* with $M = 2$.

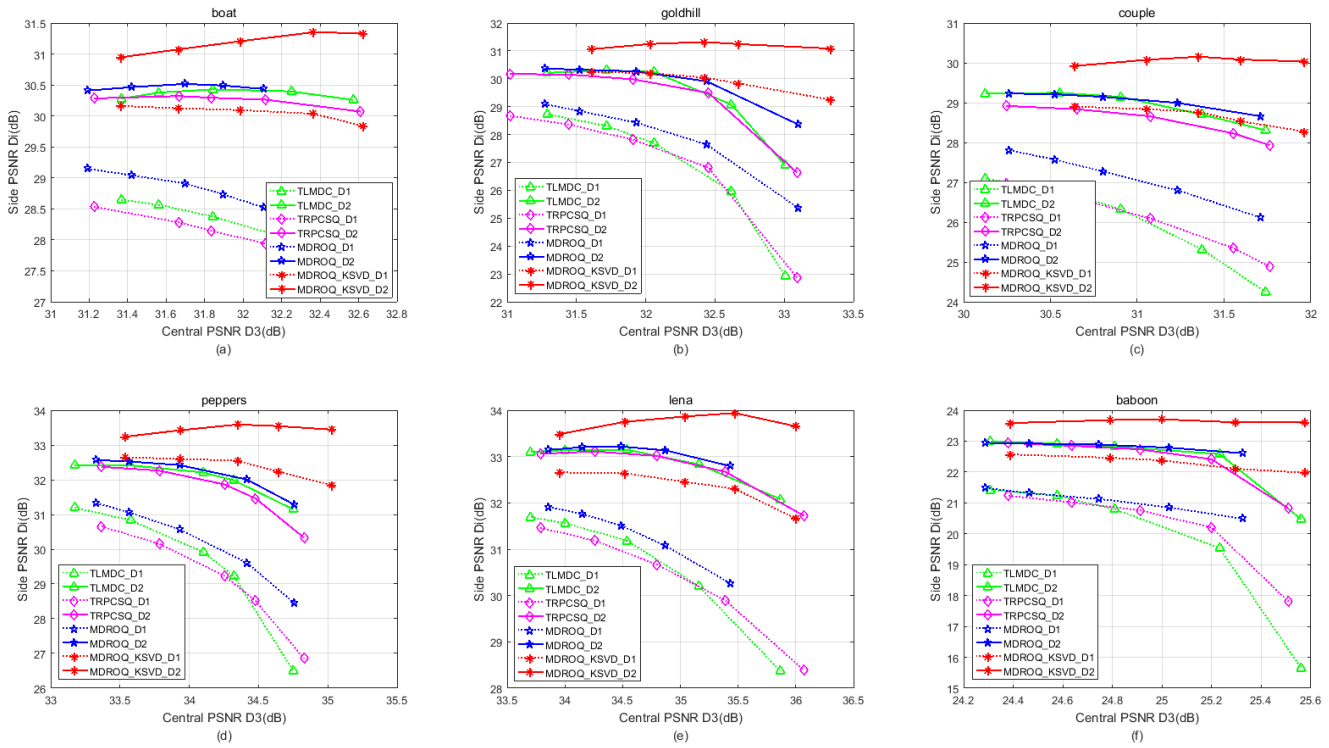

FIGURE 8. The side PSNR and central PSNR of KSVD-based MDROQ, MDROQ, TRPCSQ and TLMDC for $R = 0.5$ *bpp* with $M = 3$.

in Fig. 7, where the total bit rate (R) is 0.5 bpp. It is obvious that the proposed scheme is far better than the MDROQ and MDLTPC method for different images.

For the three-description image coding, the comparison results of KSVD-based MDROQ with MDROQ, TRPCSQ [14] and TLMDC [15] for $R = 0.5$ bpp and the

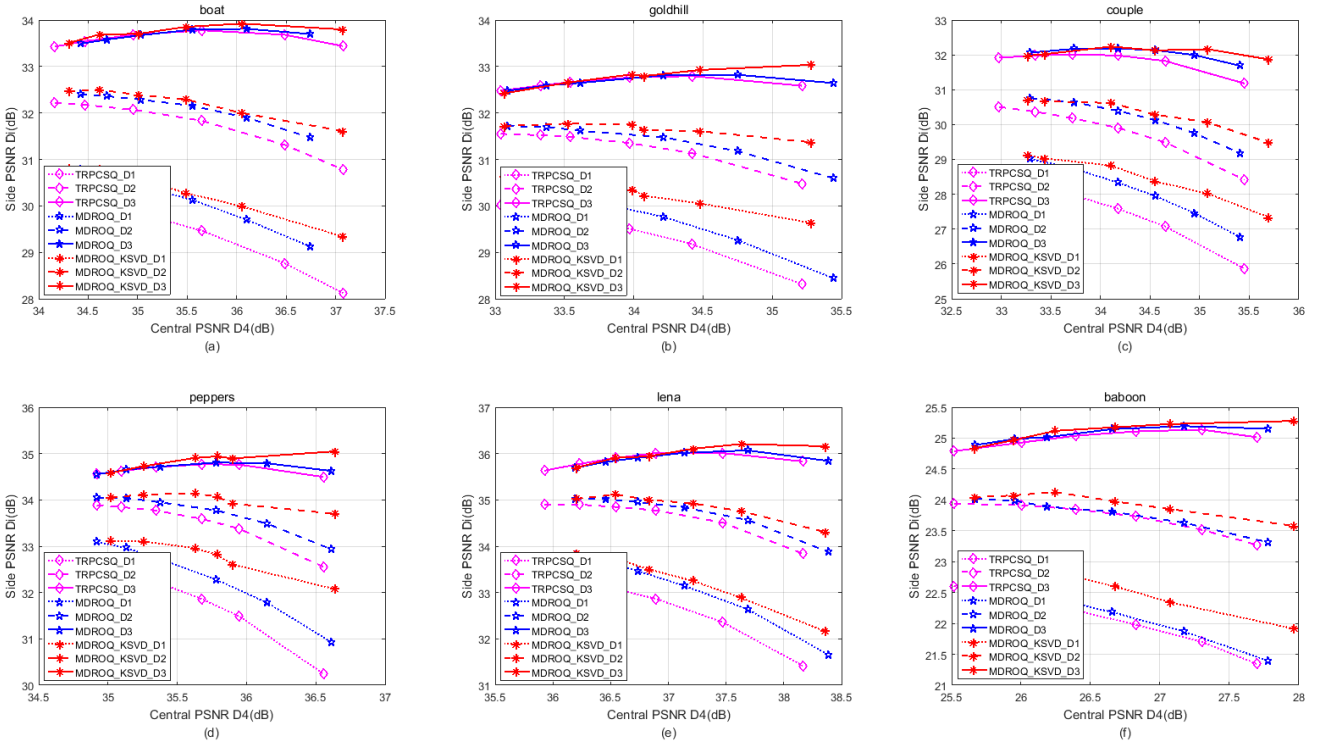

FIGURE 9. The side PSNR and central PSNR of KSVD-based MDROQ, MDROQ and TRPCSQ for $R = 1.0$ *bpp* with $M = 4$.

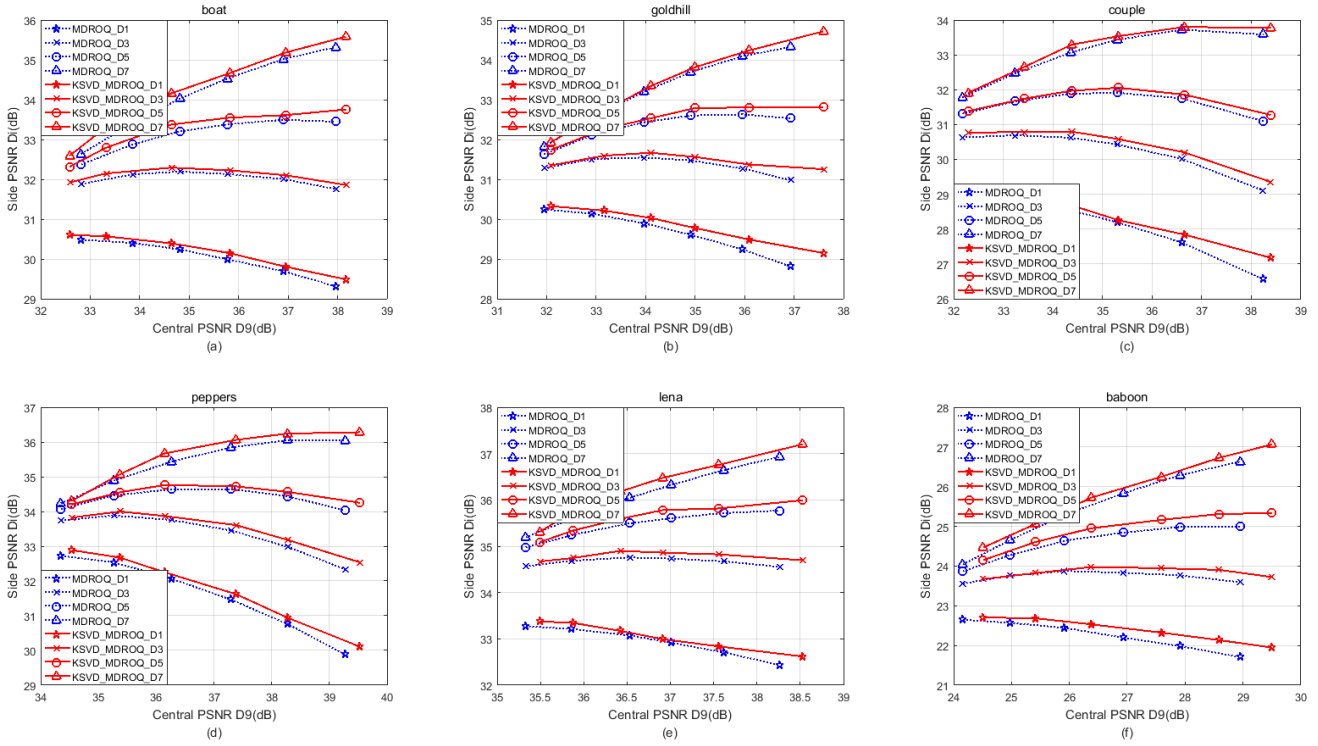

FIGURE 10. The side PSNR ($D1$, $D3$, $D5$, $D7$) and central PSNR of KSVD-based MDROQ and MDROQ for $R = 2.0$ *bpp* with $M = 9$.

comparison results of KSVD-based MDUOQ with MDUOQ, TRPCSQ and TLMDC for $R = 1$ bpp are displayed in Fig. 8 and Fig. 12, respectively. Although the third layer has been added to TLMDC, the improved methods can also be added, so they can be compared together. And our new scheme has better overall performance.

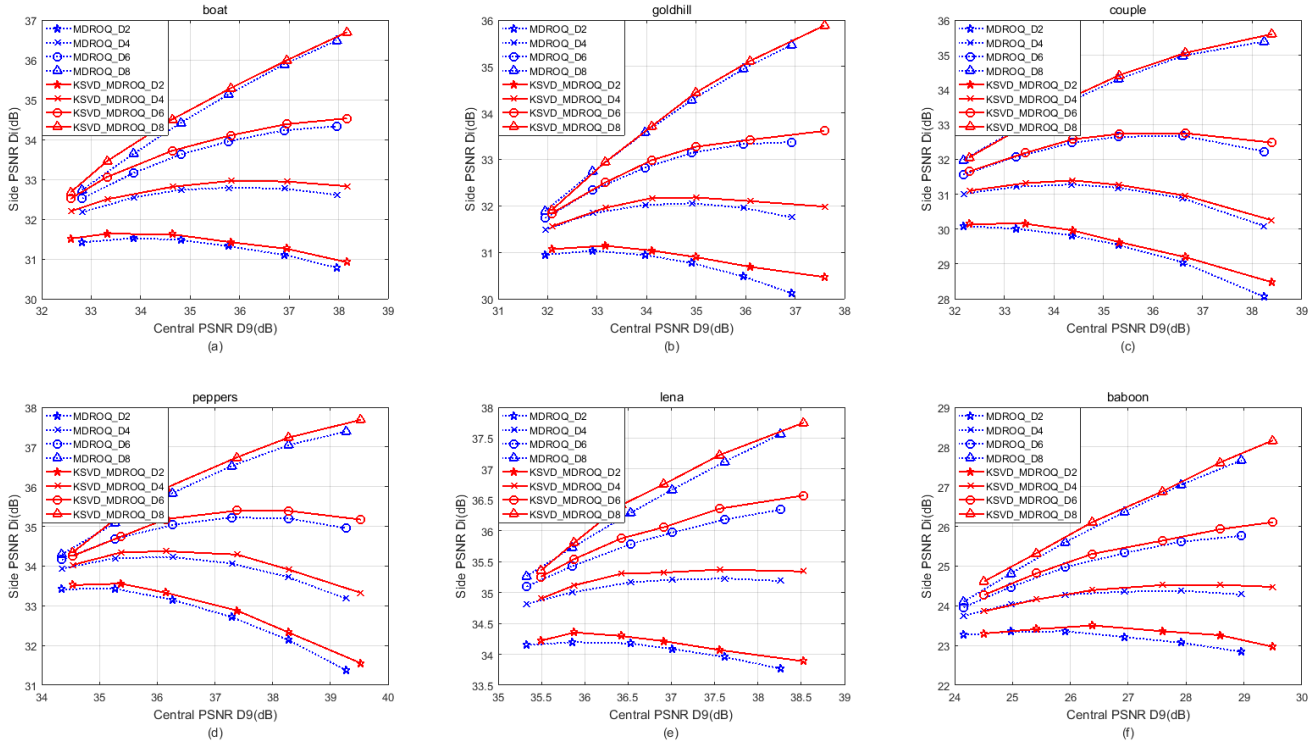

FIGURE 11. The side PSNR (*D2*, *D4*, *D6*, *D8*) and central PSNR of KSVD-based MDROQ and MDROQ for $R = 2.0$ *bpp* with $M = 9$.

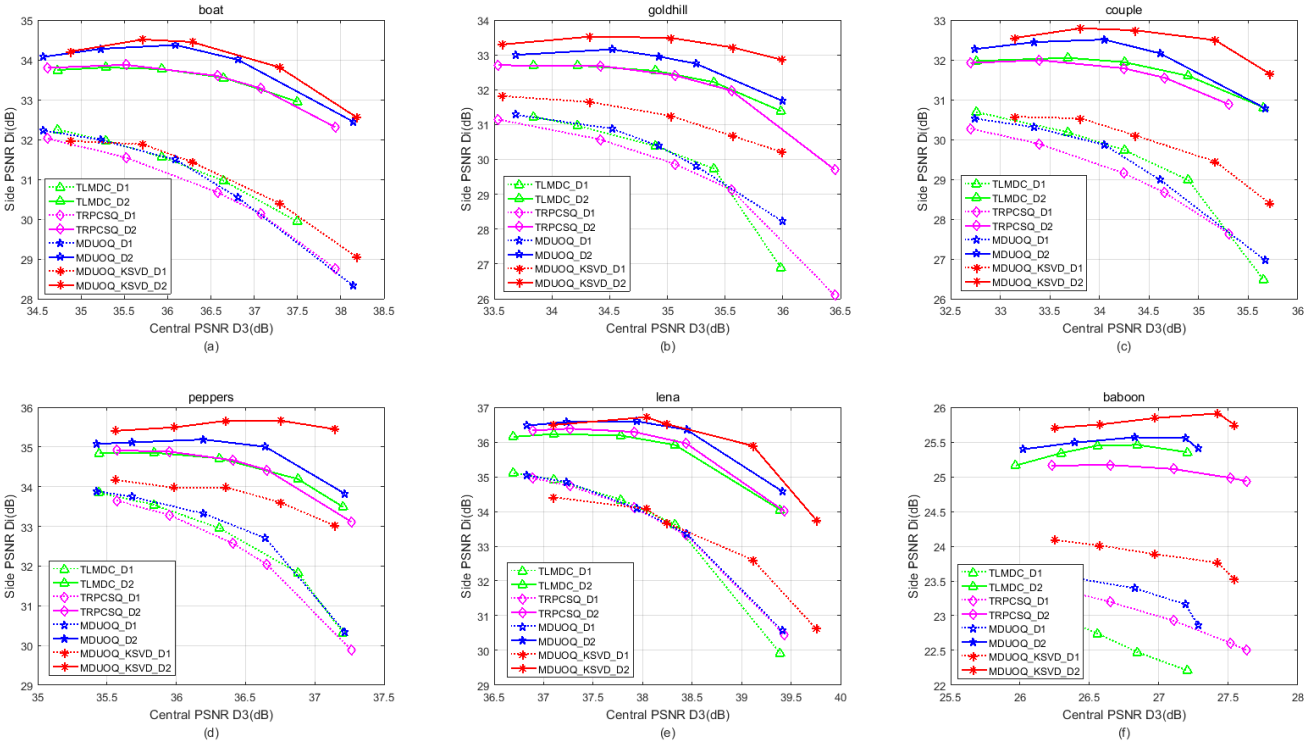

FIGURE 12. The side PSNR and central PSNR of KSVD-based MDUOQ, MDUOQ, TRPCSQ and TLMDC for $R = 1.0$ *bpp* with $M = 3$.

Fig. 9 compares the side PSNR D_i and central PSNR D_M of the four-description KSVD-based MDROQ, MDROQ and TRPCSQ with $R = 1$ bpp and Fig. 13 demonstrates the comparison results of four-description KSVD-based MDUOQ, MDUOQ and TRPCSQ. For the nine-description image coding, we separately show the results of side PSNR

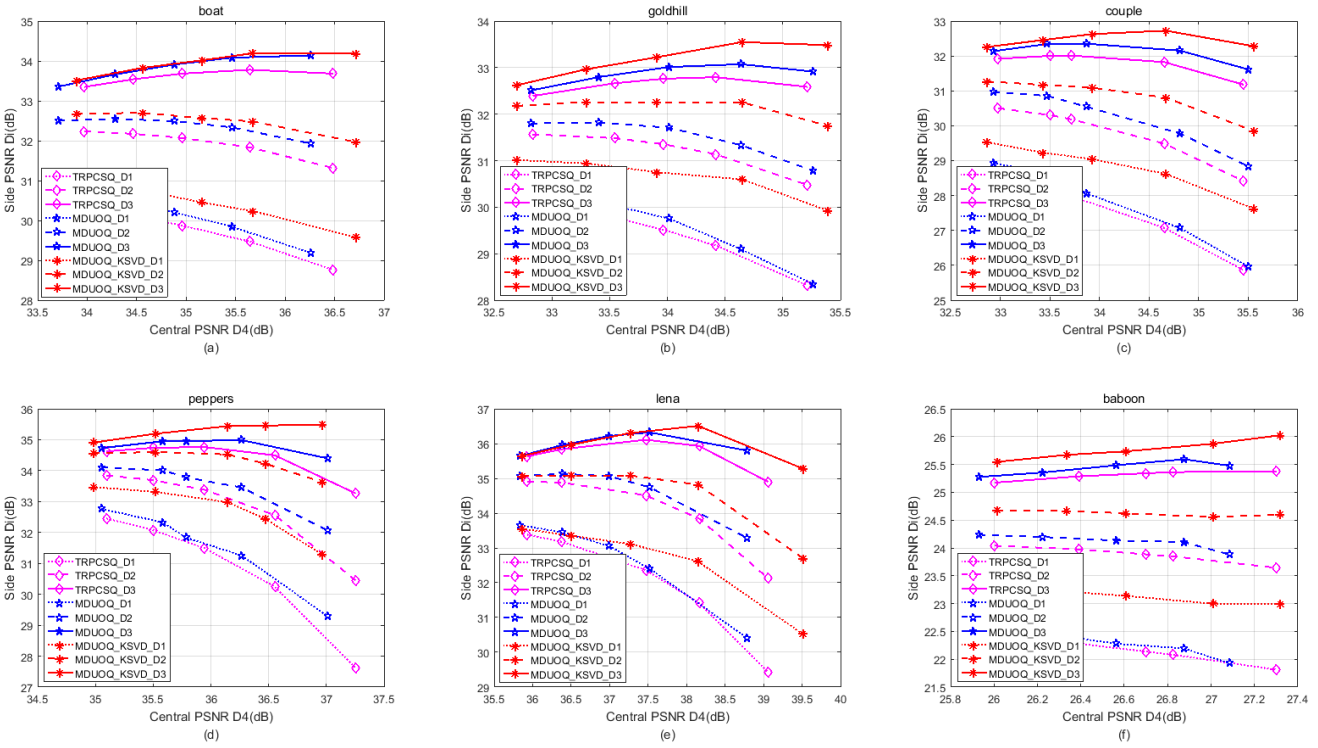

FIGURE 13. The side PSNR and central PSNR of KSVD-based MDUOQ, MDUOQ and TRPCSQ for $R = 1.0$ *bpp* with $M = 4$.

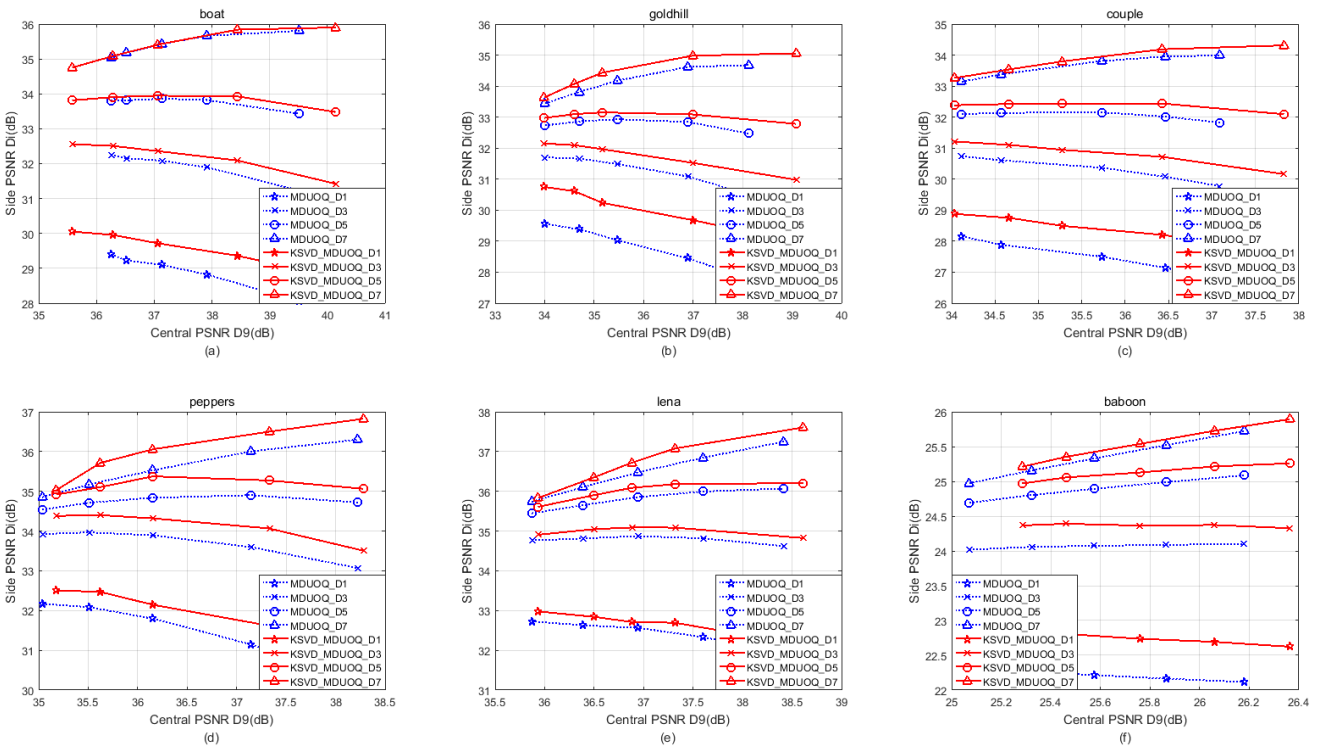

FIGURE 14. The side PSNR ($D1$, $D3$, $D5$, $D7$) and central PSNR of KSVD-based MDUOQ and MDUOQ for $R = 2.0$ *bpp* with $M = 9$.

and central PSNR with $R = 2$ bpp of KSVD-based MDROQ and MDROQ in Fig. 10 and Fig. 11 in order to avoid too crowd and the results of KSVD-based MDUOQ and MDUOQ in Fig. 14 and Fig. 15. It can be seen that the side PSNR has a greater improvement as the central PSNR increases.

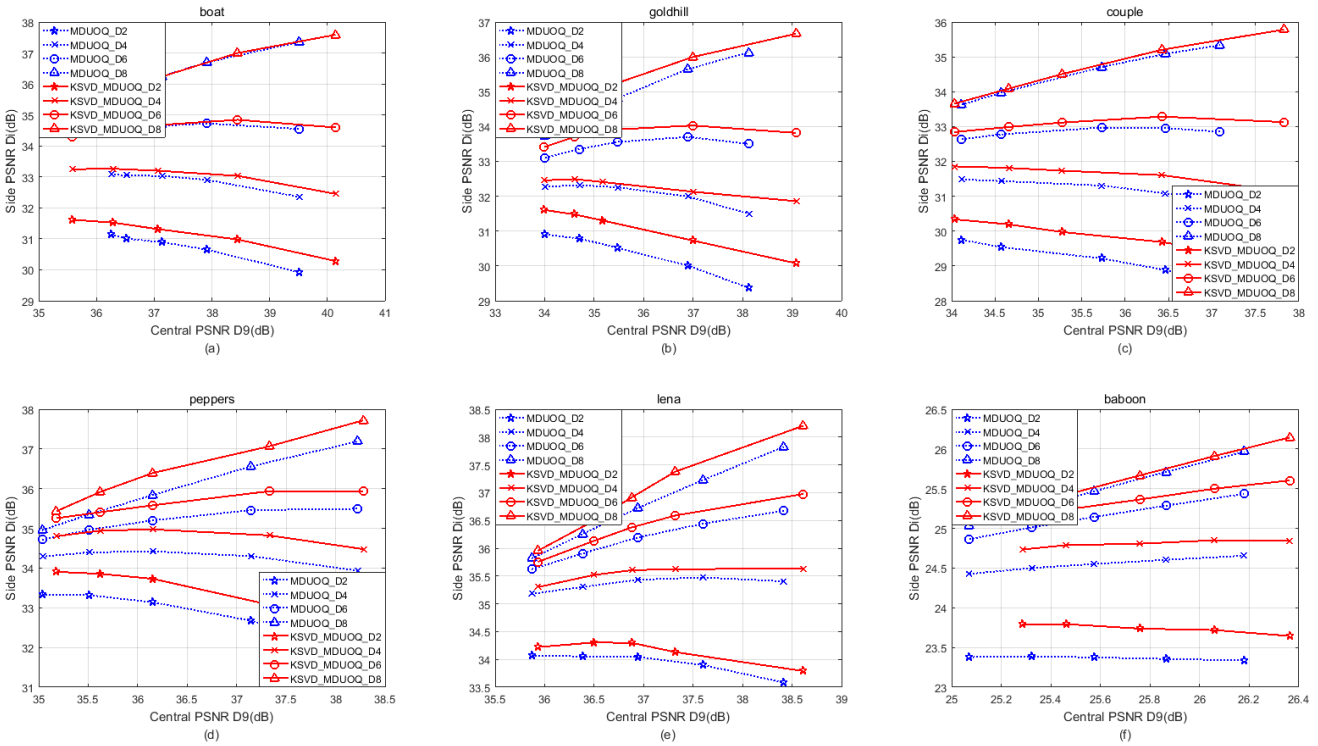

FIGURE 15. The side PSNR ($D2, D4, D6, D8$) and central PSNR of KSVD-based MDUOQ and MDUOQ for $R = 2.0$ *bpp* with $M = 9$.

From these figures, they clearly show that the proposed KSVD-based MDROQ and KSVD-based MDUOQ schemes outperform MDROQ and MDUOQ in both side PSNR and central PSNR for $M = 2, M = 3, M = 4$ *and* $M = 9$. This is because KSVD-based sparse transformation can better represent the structural characteristics of the image to improve the reconstruction quality. By observing the Fig. 9 to Fig. 11 and Fig. 13 to Fig. 15, we can also see that the proposed scheme has a better effect on MDUOQ than MDROQ for same M. Therefore, the solution we propose has a significant improvement for most images.

V. CONCLUSION

In this paper, new multiple description coding methods KSVD-based MDROQ and KSVD-based MDUOQ are proposed. The KSVD algorithm is used to achieve the sparse transform. The input source can obtain sparse transform coefficients through KSVD-based transform to improve the reconstruction accuracy. Theoretical analyses and experimental results demonstrate that the proposed scheme achieves better performance than other methods.

REFERENCES

[1] V. K. Goyal, "Multiple description coding: Compression meets the network," *IEEE Signal Process. Mag.*, vol. 18, no. 5, pp. 74–93, Sep. 2001.

[2] J. K. Wolf, A. D. Wyner, and J. Ziv, "Source coding for multiple descriptions," *Bell Syst. Tech. J.*, vol. 59, no. 8, pp. 1417–1426, Oct. 1980.

[3] V. A. Vaishampayan, "Design of multiple description scalar quantizers," *IEEE Trans. Inf. Theory*, vol. 39, no. 3, pp. 821–834, May 1993.

[4] T. Y. Berger-Wolf and E. M. Reingold, "Index assignment for multichannel communication under failure," *IEEE Trans. Inf. Theory*, vol. 48, no. 10, pp. 2656–2668, Oct. 2002.

[5] C. Tian and S. S. Hemami, "Sequential design of multiple description scalar quantizers," in *Proc. Data Compress. Conf. (DCC)*, Mar. 2004, pp. 32–41.

[6] J. Ostergaard, J. Jensen, and R. Heusdens, "n-channel entropy-constrained multiple-description lattice vector quantization," *IEEE Trans. Inf. Theory*, vol. 52, no. 5, pp. 1956–1973, May 2006.

[7] M. Liu and C. Zhu, "M-description lattice vector quantization: Index assignment and analysis," *IEEE Trans. Signal Process.*, vol. 57, no. 6, pp. 2258–2274, Jun. 2009.

[8] Y. Wang, M. T. Orchard, V. Vaishampayan, and A. R. Reibman, "Multiple description coding using pairwise correlating transforms," *IEEE Trans. Image Process.*, vol. 10, no. 3, pp. 351–366, Mar. 2001.

[9] K. Khelil, R. E. H. Bekka, A. Djebari, and J. M. Rouvaen, "Multiple description wavelet-based image coding using correlating transforms," *AEU—Int. J. Electron. Commun.*, vol. 61, no. 6, pp. 411–417, Jun. 2007.

[10] L. Li and C. Cai, "Multiple description image coding using dual-tree discrete wavelet transform," in *Proc. Int. Symp. Intell. Signal Process. Commun. Syst. (ISPACS)*, vol. 17, Jan. 2009, pp. 655–658.

[11] K. Khelil, A. Hussain, R. E. Bekka, and F. Berrezzek, "Improved multiple description wavelet based image coding using subband uniform quantization," *AEU—Int. J. Electron. Commun.*, vol. 65, no. 11, pp. 967–974, Nov. 2011.

[12] X. Liu, X. Wu, and D. Zhao, "Multiple description image coding with local random measurements," in *Proc. Data Compress. Conf.*, Mar. 2014, pp. 123–132.

[13] G. Sun, U. Samarawickrama, J. Liang, C. Tian, C. Tu, and T. D. Tran, "Multiple description coding with prediction compensation," *IEEE Trans. Image Process.*, vol. 18, no. 5, pp. 1037–1047, May 2009.

[14] U. Samarawickrama, J. Liang, and C. Tian, "M-channel multiple description coding with two-rate predictive coding and staggered quantization," *IEEE Trans. Circuits Syst. Video Technol.*, vol. 20, no. 7, pp. 933–944, Jul. 2010.

[15] U. Samarawickrama, J. Liang, and C. Tian, "A three-layer scheme for M-channel multiple description image coding," *Signal Process.*, vol. 91, no. 10, pp. 1261–1264, Oct. 2011.

[16] L. Meng, J. Liang, U. Samarawickrama, Y. Zhao, H. Bai, and A. Kaup, "Multiple description coding with randomly and uniformly offset quantizers," *IEEE Trans. Image Process.*, vol. 23, no. 2, pp. 582–595, Feb. 2014.
[17] V. K. Goyal, "Scalar quantization with random thresholds," *IEEE Signal Process. Lett.*, vol. 18, no. 9, pp. 525–528, Sep. 2011.
[18] A. Naimi and K. Belloulata, "Multiple description image coding using contourlet transform," in *Proc. 4th Int. Conf. Elect. Eng. (ICEE)*, Dec. 2015, pp. 1–4.
[19] C. Cai, J. Chen, and H. Zeng, "Multiple description coding based on enhanced X-tree," in *Proc. 6th Int. Conf. Image Process. Theory Tools Appl. (IPTA)*, Dec. 2016, pp. 1–4.
[20] L. Wang, X. Wu, and G. Shi, "Multiple description video coding against both erasure and bit errors by compressive sensing," in *Proc. Vis. Commun. Image Process. (VCIP)*, Nov. 2011, pp. 1–4.
[21] Y. Wang, A. R. Reibman, M. T. Orchard, and H. Jafarkhani, "An improvement to multiple description transform coding," *IEEE Trans. Signal Process.*, vol. 50, no. 11, pp. 2843–2854, Nov. 2002.
[22] T. D. Tran, J. Liang, and C. Tu, "Lapped transform via time-domain pre- and post-filtering," *IEEE Trans. Signal Process.*, vol. 51, no. 6, pp. 1557–1571, Jun. 2003.
[23] J. Liang, X. Li, G. Sun, and T. D. Tran, "Two-dimensional wiener filters for error resilient time domain lapped transform," in *Proc. IEEE Int. Conf. Acoust. Speech Signal Process.*, vol. 3, May 2006, p. III.
[24] J. Liang, C. Tu, L. Gan, T. D. Tran, and K.-K. Ma, "Wiener filter-based error resilient time-domain lapped transform," *IEEE Trans. Image Process.*, vol. 16, no. 2, pp. 491–502, Feb. 2007.
[25] M. Aharon, M. Elad, and A. Bruckstein, "*K*-SVD: An algorithm for designing overcomplete dictionaries for sparse representation," *IEEE Trans. Signal Process.*, vol. 54, no. 11, pp. 4311–4322, Nov. 2006.
[26] S. G. Mallat and Z. Zhang, "Matching pursuits with time-frequency dictionaries," *IEEE Trans. Signal Process.*, vol. 41, no. 12, pp. 3397–3415, Dec. 1993.
[27] S. Chen, S. A. Billings, and W. Luo, "Orthogonal least squares methods and their application to non-linear system identification," *Int. J. Control*, vol. 50, no. 5, pp. 1873–1896, May 1989.
[28] J. A. Tropp, "Greed is good: Algorithmic results for sparse approximation," *IEEE Trans. Inf. Theory*, vol. 50, no. 10, pp. 2231–2242, Oct. 2004.
[29] A. Kaur and S. Budhiraja, "Wavelet based sparse image recovery via orthogonal matching pursuit," in *Proc. Recent Adv. Eng. Comput. Sci. (RAECS)*, Mar. 2014, pp. 1–5.
[30] Y. Wang, H. Zhang, and F. Yang, "A weighted sparse neighbourhood-preserving projections for face recognition," *IETE J. Res.*, vol. 63, no. 3, pp. 1–10, Jan. 2017.

GUINA SUN received the bachelor's degree in computer science and technology from Hainan Normal University, Haikou, China, in 2016. She is currently pursuing the master's degree in computer software and theory with Shandong Normal University, Jinan, China. Her current research interests include image and video compression.

LILI MENG received the B.E. degree from Shandong University, Jinan, China, in 2005, and the Ph.D. degree from Beijing Jiaotong University, Beijing, China, in 2013, under the supervision of Prof. Yao Zhao. In 2010, she visited the National Kaohsiung University of Applied Sciences, Taiwan. From 2010 to 2011, she was a Visiting Student at Simon Fraser University, Canada, where she was a Visiting Scholar, from 2017 to 2018. She is with the School of Information Science and Engineering, Shandong Normal University. Her research interests include image/video coding and machine learning.

LI LIU received the Ph.D. degree from Shandong University, where she was involved in computer vision research. She is currently an Associate Professor of information science and engineering with Shandong Normal University. Her research interests include video and image processing, computer vision, and pattern recognition.

YANYAN TAN received the Ph.D. degree in intelligent information processing from Xidian University, Xi'an, China, in 2013. She is currently a Lecturer with the School of Information Science and Engineering, Shandong Normal University, Jinan, China. Her main research interests include computational intelligence, multi-objective optimization, data analysis, and machine learning.

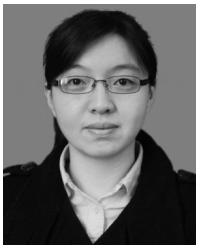

JIA ZHANG received the B.E. and M.E. degrees from the School of Underwater Acoustic Engineering, Harbin Engineering University, Harbin, China, in 2006 and 2009, respectively, and the Ph.D. degree in communication and information systems from Shandong University, in 2013. She is with the School of Information Science and Engineering, Shandong Normal University, Jinan, China. Her research interests include MIMO radio techniques, joint resource allocation and optimization in multicell cellular networks, dynamic programming, and interference coordination in heterogeneous cellular networks.

HUAXIANG ZHANG received the Ph.D. degree from Shanghai Jiaotong University, in 2004. He was an Associate Professor with the Department of Computer Science, Shandong Normal University, China, from 2004 to 2005. He is currently a Professor with the School of Information Science and Engineering and the Institute of Data Science and Technology, Shandong Normal University. He has authored over 160 journal and conference papers and has been granted nine invention patents. His current research interests include machine learning, pattern recognition, evolutionary computation, cross-media retrieval, and web information processing.